Inorganic Chemistry

Article

pubs.acs.org/IC

Steric Modifications Tune the Regioselectivity of the Alkane Oxidation Catalyzed by Non-Heme Iron Complexes

Yu He, John D. Gorden, and Christian R. Goldsmith*

Department of Chemistry and Biochemistry, Auburn University, Auburn, Alabama 36849, United States

Supporting Information

ABSTRACT: Iron complexes with the tetradentate N-donor ligand *N*,*N*′-di(phenylmethyl)-*N*,*N*′-bis(2-pyridinylmethyl)-1,2-cyclohexanediamine (bbpc) are reported. Despite the benzyl groups present on the amines, the iron compounds catalyze the oxygenation of cyclohexane to an extent similar to those employing less sterically encumbered ligands. The catalytic activity is strongly dependent on the counterion, with the highest activity and the strongest preference for alkane hydroxylation correlating to the most weakly coordinating anion, SbF_6^-. The selectivity for the alcohol product over the ketone is amplified when acetic acid is present as an additive. When hydrocarbon substrates with both secondary and tertiary carbons are oxidized by H_2O_2, the catalyst directs oxidation toward the secondary carbons to a greater degree than other previously reported iron-containing homogeneous catalysts.

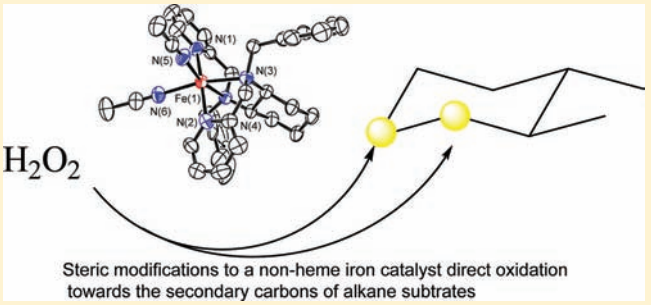

INTRODUCTION

The selective activation of C−H bonds within either a single substrate or a group of substrates remains an elusive goal in homogeneous catalysis.[1−5] With heterogeneous catalysts, the reactive portions can be encapsulated within a porous solid support. When these pores are sufficiently small, they can exclude substrates, or portions of substrates, on the bases of their size and shape.[6−10] In two recent studies with homogeneous catalysis, regioselective oxidation was achieved by engineering noncovalent interactions between a functional group on the substrate and a docking group on the catalyst.[11,12] The rigidity of the catalyst−substrate adduct is essential toward directing the oxidation toward the target region of the substrate.

The development of homogeneous catalysts for the regioselective activation of nonfunctionalized alkanes and alkenes has had less success.[13−17] One design strategy, partly influenced by the active sites of metalloenzymes,[18] is to install steric bulk onto the organic component of the catalyst, using steric repulsions to restrict the access of substrates to the reactive portion of the oxidant. If the steric bulk is the wrong size or in the wrong position, however, its placement can severely impede or eliminate the desired reactivity.[19] In some cases, this can be beneficial, for such ligand modifications have allowed the isolation of a number of reactive species relevant to nonheme iron chemistry.[20−28] A second drawback is that the addition of steric bulk can also facilitate one or more competing modes of reactivity, for instance, promoting alkene bishydroxylation over epoxidation.[29] Despite these potential problems, this strategy has been successfully applied to modulate the selectivity of hydroxylation catalyzed by iron porphyrin compounds.[30,31]

In order to alter the regioselectivity of nonheme iron catalysis, we have modified the bpmcn framework (Scheme 1),[32] replacing the methyl groups on the amine nitrogens with benzyl groups (Scheme 2). Iron(II) complexes with a similarly modified bpmen ligand retained their ability to catalyze alkane oxygenation.[33] We prepared bbpc complexes with three iron(II) salts: $FeCl_2$, $Fe(OTf)_2$, and $Fe(SbF_6)_2$. All three complexes catalyze the oxidation of alkanes by H_2O_2, with the hexafluoroantimonate salt associated with both the highest activity and the greatest selectivity for alkane hydroxylation. The bulk installed on the ligand appears to direct the oxidation toward the less sterically congested portions of substrates to an

Scheme 1

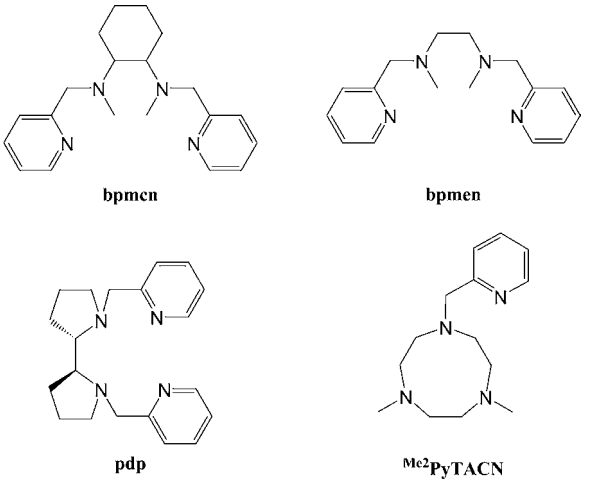

Received: August 4, 2011
Published: November 9, 2011

Scheme 2

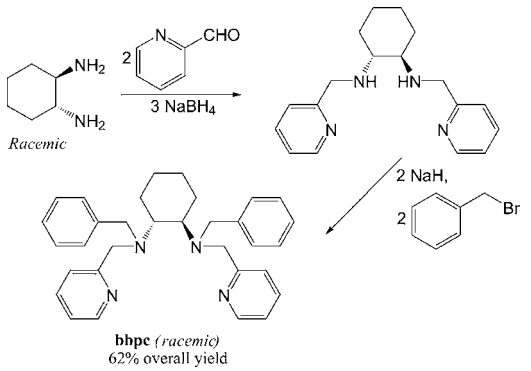

extent heretofore unobserved with mononuclear nonheme iron catalysts.

EXPERIMENTAL SECTION

Materials. Unless stated otherwise, all chemicals were purchased from Sigma-Aldrich and used as received. Anhydrous acetonitrile (MeCN) was stored in a glovebox free of moisture and oxygen. Anhydrous methanol (MeOH) and tetrahydrofuran (THF) were stored over 4 Å molecular sieves. Anhydrous diethyl ether (ether) and ammonium hydroxide (NH_4OH) were purchased from Fisher Scientific and stored in a dry, anaerobic glovebox. Silver(I) hexafluoroantimonate ($AgSbF_6$) was stored in a dark −35 °C freezer in a dry, anaerobic glovebox. Chloroform-*d* ($CDCl_3$), acetonitrile-d_3 (CD_3CN), and cyclohexane-d_{12} (C_6D_{12}) were bought from Cambridge Isotopes. Ethanol (EtOH) was purchased from Fluka. Iron(II) triflate ($Fe(OTf)_2{\cdot}2MeCN$) was prepared through a previously reported procedure,[34] as were *N,N′*-dimethyl-*N,N′*-bis(2-pyridinylmethyl)-1,2-ethanediamine (bispicen) and *N,N′*-dimethyl-*N,N′*-bis(2-pyridinylmethyl)-1,2-cyclohexanediamine (bpmcn).[35] The $[Fe(bpmcn)(MeCN)_2](SbF_6)_2$ complex was prepared from the reaction of $[Fe(bpmcn)Cl_2]$ with 2 equiv of $AgSbF_6$ in MeCN; the dication was confirmed to be the *cis-α* isomer on the basis of its ^1H NMR and optical spectra.[32]

Instrumentation. ^1H and ^{13}C nuclear magnetic resonance (NMR) spectra were recorded on either a 400 MHz or a 250 MHz AV Bruker NMR spectrometer at 22 °C. All NMR peaks were referenced to internal standards. A Varian Cary 50 spectrophotometer was used to collect optical data, which were processed and analyzed using software from the WinUV Analysis Suite. A Johnson Matthey magnetic susceptibility balance (model MK I#7967) was used to measure the magnetic moments of solid samples. High resolution mass spectrometry (HR-MS) data were acquired at the Mass Spectrometer Center at Auburn University on a Bruker microflex LT MALDI-TOF mass spectrometer via direct probe analysis operated in the positive ion mode. Electron paramagnetic resonance (EPR) spectra were collected on a Bruker EMX-6/1 X-band EPR spectrometer operated in the perpendicular mode. All EPR spectra were analyzed with the program EasySpin.[36] All EPR samples were run as frozen MeCN solutions in quartz tubes. Crystalline samples were dried and sent to Atlantic Microlabs (Norcross, GA) for elemental analysis.

X-Ray Crystallography. X-ray diffraction data were collected at −80 °C on a Bruker SMART APEX CCD X-ray diffractometer unit using Mo Kα radiation from crystals mounted in Paratone-N oil on glass fibers. SMART (v 5.624) was used for preliminary determination of cell constants and data collection control. Determination of integrated intensities and global cell refinement were performed with the Bruker SAINT software package using a narrow-frame integration algorithm. The program suite SHELXTL (v 5.1) was used for space group determination, structure solution, and refinement.[37] Refinement was performed against F^2 by weighted full-matrix least-squares, and empirical absorption correction (SADABS) were applied.[38] Hydrogen atoms were placed at calculated positions using suitable riding models with isotropic displacement parameters derived from their carrier atoms. Crystallographic data and selected bond distances and angles are provided in Tables 1 and 2 and Table S1 of the Supporting Information.

Synthesis. *N,N′-Di(phenylmethyl)-N,N′-bis(2-pyridinylmethyl)-1,2-cyclohexanediamine (bbpc).* 2-Pyridinecarboxaldehyde (4.551 g, 42.5 mmol) was added to a solution of (±)-*trans*-1,2-diaminocyclohexane (2.422 g, 21.2 mmol) in 40 mL of dry MeOH. The reaction mixture stirred at 60 °C for 2 h, at which point sodium borohydride (4.848 g, 128 mmol) was added as a solid. The resultant mixture was heated at reflux for 16 h, at which point the reaction was cooled and the MeOH removed under reduced pressure, yielding crude *N,N′*-bis(2-pyridinylmethyl)-1,2-cyclohexanediamine. The crude material was dissolved in distilled H_2O, at which point the precursor was extracted with 4 × 100 mL portions of CH_2Cl_2. These extracts were dried over Na_2SO_4. Removal of the CH_2Cl_2 under reduced pressure yielded the purified *N,N′*-bis(2-pyridinylmethyl)-1,2-cyclohexanediamine as a yellow oil (5.556 g, 18.8 mmol, 88%). The compound's purity and identity were confirmed by ^1H NMR.[39] The precursor (1.603 g, 5.42 mmol) was dissolved in 60 mL of dry THF. The solution was cooled to 0 °C, at which point, sodium hydride (2.067 g,

Table 1. Selected Crystallographic Data for the bbpc Complexes

parameter	$[Fe(bbpc)Cl_2]{\cdot}MeCN$	$[Fe(bbpc)(MeCN)_2](SbF_6)_2$	$[Fe(bbpc)(OTf)_2]$
formula	$C_{34}H_{39}Cl_2FeN_5$	$C_{36}H_{42}FeF_{12}N_6Sb_2$	$C_{34}H_{34}F_6FeN_4O_6S_2$
MW	644.45	1086.13	830.66
cryst syst	orthorhombic	orthorhombic	triclinic
space group	$P2_12_12_1$ (#19)	$P2_12_12_1$ (#19)	$P\bar{1}$(#2)
a (Å)	10.3299(10)	14.9875(7)	10.2508(11)
b (Å)	16.3604(16)	16.5523(8)	11.8558(12)
c (Å)	18.4921(18)	19.8461(10)	15.8754(16)
α (deg)	90	90	71.418(2)
β (deg)	90	90	85.954(2)
γ (deg)	90	90	76.263(2)
V (Å^3)	3125.2(5)	4923.4(4)	1776.4(3)
Z	4	4	2
cryst color	dark red	green	yellow
T (K)	193	193	193
reflns collected	48351	12228	11965
unique reflns	11128	9116	5925
R1 (F, I > 2σ(I))[a]	0.0509	0.048	0.0585
wR2 (F^2, all data)[a]	0.1018	0.1155	0.1879

[a] $R1 = \sum||F_o| - |F_c||/\sum|F_o|$; $wR2 = [\sum w(F_o^2 - F_c^2)^2/\sum w(F_o^2)^2]^{1/2}$.

dx.doi.org/10.1021/ic201695a | *Inorg. Chem.* 2011, 50, 12651–12660

Table 2. Selected Bond Lengths for Fe(II) Complexes with the bbpc Ligand, $[Fe(bbpc)X_2]^{n+}$ (Å)[a]

X =	Cl	MeCN	OTf
Fe–N(1)	2.2224(15)	2.146(4)	2.146(3)
Fe–N(2)	2.1798(16)	2.182(4)	2.132(3)
Fe–N(3)	2.3286(15)	2.227(3)	2.234(3)
Fe–N(4)	2.4391(16)	2.256(3)	2.225(3)
Fe–X(1)	2.3608(5)	2.147(4)	2.270(2)
Fe–X(2)	2.4708(6)	2.164(4)	2.107(3)

[a]Donor atoms have been relabeled from their CIF designations to facilitate comparison. N(1) and N(2) correspond to pyridine nitrogens; N(3) and N(4) correspond to amine nitrogens.

51.7 mmol) was added as a solid. After stirring for 20 min, benzyl bromide (1.949 g, 11.4 mmol) was added at 0 °C. The reaction was warmed to room temperature and stirred for an additional 48 h. Water was added dropwise to quench the reaction. Subsequently, 3 M HCl was added dropwise until the pH of the aqueous layer fell beneath 2. The organic layer was removed under reduced pressure, and the remaining acidic layer was washed with 3 × 40 mL aliquots of ether. The aqueous solution was made basic (pH > 10) through the addition of 3 M NaOH, at which point, the product was extracted with 3 × 100 mL portions of ethyl acetate (EtOAc). The collected EtOAc layers were dried over Na_2SO_4, filtered, and concentrated to yield the crude product as a brown oil. The pure ligand may be obtained through flash chromatography on silica with a 20:4:1 mixture of EtOAc/EtOH/NH_4OH as the elutant (R_f = 0.89). Alternatively, the ligand can be obtained in crystalline form by cooling a saturated solution of the crude in MeCN. The latter process affords a higher yield of the light yellow product (1.814 g, 3.81 mmol, 70%). ^{1}H NMR ($CDCl_3$, 400 MHz): δ 8.50 (m, 2H), 7.71 (m, 2H), 7.49 (t, 2H), 7.34 (m, 4H), 7.18–7.09 (m, 8H), 3.73 (q, 4H), 3.49 (q, 4H), 2.70 (m, 2H), 2.14 (m, 2H), 1.72 (m, 2H), 1.06 (4H). ^{13}C NMR ($CDCl_3$, 62.5 MHz): δ 161.32, 148.84, 140.11, 136.10, 129.11, 128.12, 126.87, 123.28, 121.77, 59.08, 55.49, 53.93, 26.03, 24.49. HR-MS (ESI) Calcd, MH^+: 477.3018. Found: 477.3017.

cis-Dichloro-(N,N′-di(phenylmethyl)-N,N′-bis(2-pyridinylmethyl)-1,2-cyclohexanediamine)manganese(II) ([Mn(bbpc)Cl$_2$]). The bbpc ligand (0.510 g, 1.07 mmol) and $MnCl_2$ (0.130 g, 1.03 mmol) were dissolved in 10 mL of MeCN and stirred for 16 h under N_2, during which time a white solid deposited. The addition of ether (5 mL) yielded more precipitate. The product was isolated through filtration as a white powder (0.310 g, 50%). Crystals suitable for analysis by X-ray diffraction were obtained through the vapor diffusion of ether into a saturated solution of the manganese complex in MeCN. Solid-state magnetic susceptibility (294 K): μ_{eff} = 5.8 μ_B. Optical spectroscopy (MeCN, 294 K): 310 nm (shoulder), 390 M^{-1} cm^{-1}. Elemental Analysis Calcd for $C_{32}H_{36}N_4MnCl_2 \cdot CH_3CN$: C, 63.45%; H, 6.11%; N, 10.88%. Found: C, 63.31%; H, 6.23%; N, 10.81%.

cis-Dichloro-(N,N′-di(phenylmethyl)-N,N′-bis(2-pyridinylmethyl)-1,2-cyclohexanediamine)iron(II) ([Fe(bbpc)Cl$_2$]). The bbpc ligand (1.07 g, 2.25 mmol) was dissolved in 5 mL of MeCN and combined with a solution of $FeCl_2$ (0.284 g, 2.23 mmol) in 5 mL of MeCN. Upon stirring for 16 h under an anaerobic atmosphere, a yellow solid began to precipitate. Ether (5 mL) was added, depositing more of the product. The product was isolated through filtration as a yellow powder (0.874 g, 65%). Crystals suitable for X-ray diffraction were grown through vapor diffusion of ether into a saturated solution of the iron complex in MeCN. Solid-state magnetic susceptibility (294 K): μ_{eff} = 4.9 μ_B. Optical spectroscopy (MeCN, 294 K): 380 nm, 1400 M^{-1} cm^{-1}. Elemental Analysis Calcd for $C_{32}H_{36}N_4FeCl_2 \cdot CH_3CN \cdot 0.5H_2O$: C, 62.49%; H, 6.17%; N, 10.72%; Found: C, 62.65%; H, 6.09%; N, 10.69%.

trans-Ditriflato-(N,N′-di(phenylmethyl)-N,N′-bis(2-pyridinylmethyl)-1,2-cyclohexanediamine)iron(II) ([Fe(bbpc)(OTf)$_2$]). The bbpc ligand (0.852 g, 1.79 mmol) and $Fe(OTf)_2 \cdot 2MeCN$ (0.782 g, 1.79 mmol) were dissolved in 5 mL of MeCN, resulting in a dark red brown solution. The reaction stirred under N_2 for 30 min, at which point the volume of MeCN was reduced through an applied vacuum. The addition of ether precipitated the product as a light yellow powder (0.696 g, 45%). Crystals suitable for X-ray diffraction were obtained through the slow addition of ether to a solution of the powder in CH_2Cl_2. ^{1}H NMR (CD_3CN, 250 MHz): δ 58.0, 57.7, 54.6, 52.7, 37.7, 22.3, 21.1, 16.0, 13.7, 10.9, 10.2, 6.4, 5.5, 5.1, 4.7, 4.4, 3.9, 3.5, 3.2, 1.0, 0.5, −0.2, −1.3, −8.0, −21.3. Solid-state magnetic susceptibility (294 K): μ_{eff} = 4.6 μ_B. Optical spectroscopy (MeCN, 294 K): 350 nm, 1600 M^{-1} cm^{-1}. Elemental Analysis Calcd for $C_{34}H_{36}N_4FeF_6O_6S_2 \cdot CH_3CN \cdot 0.5H_2O$: C, 48.64%; H, 4.44%; N, 6.67%. Found: C, 48.36%; H, 4.27%; N, 6.74%.

cis-Diacetonitrilo-(N,N′-di(phenylmethyl)-N,N′-bis(2-pyridinylmethyl)-1,2-cyclohexanediamine)iron(II) Hexafluoroantimonate ([Fe(bbpc)(CH$_3$CN)$_2$](SbF$_6$)$_2$). The synthesis is based on a literature procedure.[13] Solid $[Fe(bbpc)Cl_2]$ (0.503 g, 0.835 mmol) was suspended in 10 mL of MeCN under N_2. As the suspension was vigorously stirred, $AgSbF_6$ (0.574 g, 1.67 mmol) was added. The mixture continued to stir in the dark for 24 h, with the reaction vessel covered with aluminum foil to further limit the exposure of the silver salts to light. At the conclusion of the reaction, the suspension was filtered through a packed Celite plug. Removal of the solvent under reduced pressure yielded a purple powder. The purple solid was redissolved in MeCN and filtered through a 0.2 μm Acrodisc LC PVDF filter (HPLC certified). The MeCN was removed through evaporation. The purple residue was treated to two more dissolution/filtration/concentration cycles to ensure the complete removal of the silver salts. The purple solid was dried under a nitrogen stream to yield $[Fe(bbpc)(CH_3CN)_2](SbF_6)_2$ (0.805 g, 89% yield). ^{1}H NMR (CD_3CN, 250 MHz): δ 62.4, 58.5, 52.5, 50.5, 26.2, 25.4, 23.6, 18.9, 14.0, 4.99, 3.7, −5.3, −12.6. Solid-state magnetic susceptibility (294 K): μ_{eff} = 4.4 μ_B. Optical spectroscopy (MeCN, 294 K): 340 nm, 1050 M^{-1} cm^{-1}. Elemental Analysis Calcd for $C_{36}H_{42}N_6FeF_{12}Sb_2$: C, 39.81%; H, 3.90%; N, 7.74%. Found: C, 40.26%; H, 3.98%; N, 8.06%.

RESULTS

Synthesis. The bbpc ligand can be prepared in moderate yield (62% over two steps) through the procedure outlined in Scheme 2. The two-step synthesis proceeds through the previously characterized *N,N′*-bis(2-pyridinylmethyl)-1,2-cyclohexanediamine.[39] Since the synthesis begins with a racemic mixture of *trans*-1,2-cyclohexanediamine, the bbpc product is also racemic. Scheme 2 shows only the *R,R* enantiomers in order to improve clarity. The final organic product can either be purified through chromatography or through direct crystallization from a solution of the crude material dissolved in MeCN. The obtained crystals are suitable for X-ray diffraction (Figure S1, Supporting Information).

The $[M(bbpc)Cl_2]$ compounds (M = Mn, Fe) were prepared by mixing MeCN solutions of bbpc and either $MnCl_2$ or $FeCl_2$. Both the Mn(II) and Fe(II) products precipitate readily from the reaction mixture. The $[Fe(bbpc)(SbF_6)_2]$ complex resulted from the reaction of $[Fe(bbpc)Cl_2]$ with $AgSbF_6$. In MeCN, acetonitrile molecules displace the weakly bound hexafluoroantimonate anions, and the isolated product is $[Fe(bbpc)(MeCN)_2](SbF_6)_2$. Although triflate ions are also widely perceived to be weakly coordinating ligands, it was the $[Fe(bbpc)(OTf)_2]$ complex that was isolated from the reaction between bbpc and $Fe(OTf)_2 \cdot 2MeCN$, as assessed by crystallography and elemental analysis.

Structural and Solid-State Characterization. The bbpc ligand and its Mn(II) and Fe(II) complexes crystallize readily from MeCN solutions (Table 1 and Table S1, Supporting Information). For $[Mn(bbpc)Cl_2]$, $[Fe(bbpc)Cl_2]$, and $[Fe(bbpc)(MeCN)_2]^{2+}$, the tetradentate ligand coordinates to the metal in a *cis-α* conformation, in which the two pyridine rings are *trans* to each other and the two chloride ligands are *cis* to

dx.doi.org/10.1021/ic201695a | Inorg. Chem. 2011, 50, 12651–12660

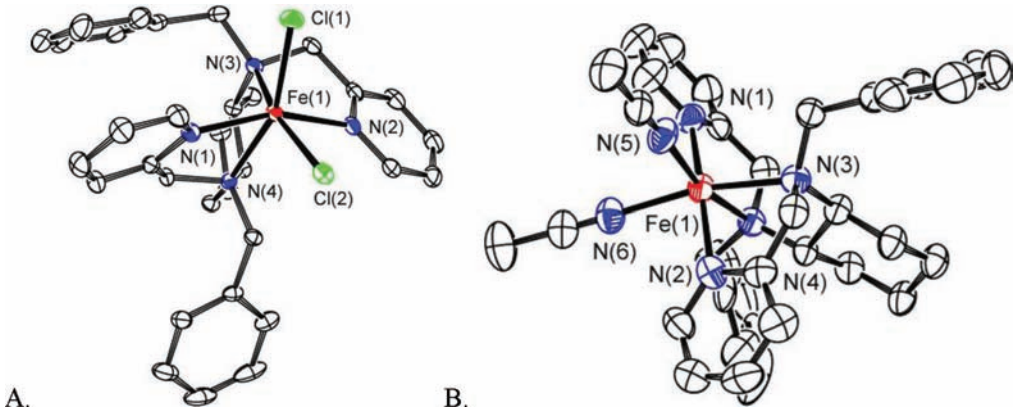

Figure 1. ORTEP representations of (A) $[Fe(bbpc)Cl_2]$ and (B) $[Fe(bbpc)(MeCN)_2]^{2+}$. The hydrogen atoms, counteranions, and outer-sphere acetonitrile molecules have been omitted for clarity. All thermal ellipsoids are drawn at 50% probability. Note that the donor atoms have been relabeled from their original CIF designations to facilitate comparison of the crystallographic data.

each other (Figure 1). Unexpectedly, the bbpc ligand is found in the *trans* conformation in the structure of the $[Fe(bbpc)(OTf)_2]$ complex (Figure 2). In this structure, one of the

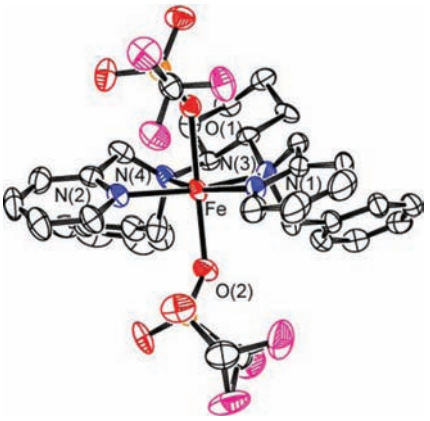

Figure 2. ORTEP representation of $[Fe(bbpc)(OTf)_2]$. Hydrogen atoms have been omitted for clarity, as have the ellipsoids for the disordered triflate and cyclohexane backbone corresponding to molecular configuration b. The disordered triflate binds to the Fe(II) ion through O(2). All thermal ellipsoids are drawn at 50% probability. Note that the donor atoms have been relabeled from their original CIF designations to facilitate comparison of the structures.

triflate anions and the cyclohexane backbone are disordered over two sets of positions; the disorder of the cyclohexane component corresponds to a mixture of (*R*,*R*) and (*S*,*S*) chiralities at carbons 1 and 2 of the ring. The chiralities of the amine nitrogens is (*R*,*S*) for both molecular configurations, resulting in a mixture of diastereomers in the crystal. The *trans* conformation has not been observed previously for *N*,*N*′-bis(2-pyridinylmethyl)-1,2-cyclohexanediamine or its close derivatives,[32] although it has been observed recently for a ligand with a 1,2-ethanediamine backbone.[40] Despite the presence of the benzyl groups, the tertiary amines remain bound to the metal ions in all four complexes.

The metal–ligand bond distances in the Fe(II) complexes are consistent with high-spin iron centers (Table 2).[41] These spin-state assignments are corroborated by solid-state magnetic susceptibility measurements. The Fe–N bond distances are notably shorter for the $[Fe(bbpc)(MeCN)_2]^{2+}$ and $[Fe(bbpc)(OTf)_2]$ complexes. In the $[Fe(bbpc)Cl_2]$ complex, the two Fe–Cl bond lengths differ by 0.11 Å. Similarly, Fe–N(4) is 0.08 Å longer than Fe–N(3) in this structure. The disparities in these bond lengths can be attributed to the different steric interactions between the two chlorides and the benzyl groups of the bbpc ligand. The benzyl group on N(4) is nearly eclipsed with the Fe–Cl(2) bond, with a dihedral angle of 11.2°. The heightened steric repulsion that results from this configuration elongates both Fe–Cl(2) and Fe–N(4). Conversely, the benzyl group on N(3) is in a staggered conformation relative to the Fe–Cl(1) bond, with a dihedral angle of 43.2°. The shorter Fe–Cl(1) and Fe–N(3) bonds are compatible with the lesser strain. The Fe–O bonds in the structure of $[Fe(bbpc)(OTf)_2]$ differ by 0.17 Å. In this structure, Fe–O(1) and the benzyl groups are on the same side of the plane defined by the four N donors. The increased steric repulsions between the O(1)-containing triflate and the benzyl groups likely explains why Fe–O(1) is longer than Fe–O(2).

Solution Characterization. Each iron complex has a single ligand-to-metal charge transfer (LMCT) band with λ_{max} between 300 and 400 nm. The energies and relatively low intensities of these bands are typical for high-spin Fe(II) complexes.[42] Solutions of all three Fe(II) compounds in CD_3CN were found to be paramagnetic by ^1H NMR, further confirming the spin states of the Fe(II) complexes. The spectra for $[Fe(bbpc)(MeCN)_2]^{2+}$ and $[Fe(bbpc)(OTf)_2]$ are consistent with the solid-state structures, with the latter containing two diastereomers. The numbers and sharpness of the peaks suggest that the conformation of the bbpc ligand is static on the NMR time-scale. The $[Fe(bbpc)Cl_2]$ complex was not sufficiently soluble in CD_3CN to unambiguously support the same conclusions. The optical spectra of the triflate and hexafluoroantimonate complexes are not identical, contrary to what would be anticipated if both counteranions were noncoordinating. In conjunction with the structural data, these results may suggest either that the *trans* conformation of $[Fe(bbpc)(OTf)_2]$ is retained in solution or that the triflates retain their stronger affinity for the Fe(II) centers in solution.

Reactivity Studies—Cyclohexane. The abilities of the three Fe(II) compounds to catalyze the oxidation of alkanes by H_2O_2 were assayed with cyclohexane in MeCN at 298 K (Table 3). The iron catalyst with the hexafluoroantimonate counteranions has the highest reactivity (TON = 27.4) and preferentially produces the alcohol product, cyclohexanol, over the ketone, cyclohexanone (A/K = 7.3). When the reactions

dx.doi.org/10.1021/ic201695a | *Inorg. Chem.* 2011, 50, 12651–12660

Table 3. Catalyzed Oxidation of Cyclohexane by Hydrogen Peroxide[a]

catalyst	$[H_2O_2]$ (mM)	$[CH_3CO_2H]$ (mM)	TON[b]	A/K[c]
$[Fe(bbpc)(Cl)_2]$	100	0	12.4	0.7
$[Fe(bbpc)(OTf)_2]$	100	0	12.8	2.6
$[Fe(bbpc)(MeCN)_2](SbF_6)_2$	10	0	4.0	7.3
$[Fe(bbpc)(MeCN)_2](SbF_6)_2$	100	0	27.4	4.8
$[Fe(bbpc)(MeCN)_2](SbF_6)_2$	100	1.0	19.0	4.7
$[Fe(bbpc)(MeCN)_2](SbF_6)_2$	10	670	2.8	12.1
$[Fe(bbpc)(MeCN)_2](SbF_6)_2$	100	670	10.9	6.8

[a]Standard reaction conditions: The starting concentrations of the iron(II) catalyst and the cyclohexane substrate in all reactivity assays were 1.0 mM and 1.0 M, respectively. All reactions were run at 298 K. A solution of H_2O_2 diluted in MeCN was added dropwise over the course of 1 min. The final volume of each reaction solution was 2.50 mL. The duration of each reaction was 30 min. After this time, the solution was filtered through silica gel and analyzed via GC. [b]Turnover number, defined as the number of moles of cyclohexanol and cyclohexanone generated per mole of Fe(II) catalyst. [c]The products were identified by GC/MS and comparison of the retention times with those of authentic samples of cyclohexanol (A) and cyclohexanone (K). The concentrations of each organic product were calibrated relative to that of an internal standard (dichlorobenzene) with a known concentration.

were run under air, the results were identical within error to those run under a dry N_2 atmosphere. Higher loadings of the terminal oxidant decrease the A/K ratio, consistent with earlier reports on related systems.[43−46] The addition of a stoichiometric amount of acetic acid (AcOH) into the system increases the selectivity for the alcohol but decreases the overall oxidative activity. This effect is not seen with a catalytic amount of AcOH. Triethylamine was also explored as an additive. When 0.40 mol of the base is present, cyclohexanone is the preferred product (A/K = 0.17), but the catalytic activity is almost completely lost (TON = 1.4).

The oxidation of cyclohexanol to cyclohexanone in the presence and absence of AcOH was monitored over 30 min (Figure 3). When AcOH is added, the number of turnovers

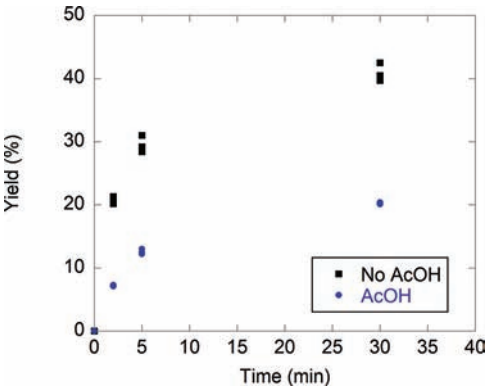

Figure 3. Oxidation of cyclohexanol in the presence and absence of acetic acid (AcOH) as a function of time. The initial concentrations of reagents were as follows: 1.0 mM $[Fe(bbpc)(MeCN)](SbF_6)_2$, 100 mM cyclohexanol, 100 mM H_2O_2, 670 mM AcOH (when present). All reactions were run in MeCN at 298 K. The yield is the amount of cyclohexanol that has been oxidized to cyclohexanone; no other organic products were observed.

completed in 30 min decreases from 41 to 20. The lifetimes of the catalytic activities under these conditions appear to be similar, with estimated half-lives of 2.4 min (AcOH absent) and 3.5 min (AcOH present).

A kinetic isotope effect of 2.4 was measured from competition studies between protonated and deuterated cyclohexane (C_6D_{12}). When C_6D_{12} is run as a substrate with 100 mM of H_2O_2, 9.6 turnovers are observed with a A/K ratio of 3.1. The lower A/K ratio suggests that the deuteration of the substrate slows the primary oxidation to the alcohol to a greater extent than the secondary step in the oxidation, which converts the alcohol to the ketone.

Reactivity Studies—1,2-Dimethylcyclohexanes and Other Sterically Complicated Alkanes. The two benzyl groups can potentially limit substrate access to the reactive portion of the oxidant, which we believe is a higher-valent iron complex (*vide infra*). The steric bulk represented by these benzyl groups could potentially hinder the oxidation of more sterically congested C−H bonds. The regioselectivity of $[Fe(bbpc)(MeCN)_2]^{2+}$ was tested using a protocol developed by Chen and White, which employs *cis*- and *trans*-1,2-dimethylcyclohexanes as diagnostic substrates.[13] The key output in these experiments is the relative prevalence of oxidation at the secondary and tertiary carbons of the two substrates. Equatorial C−H bonds tend to be more readily oxidized than axial C−H bonds in cyclohexane rings.[48] The *trans* isomer of 1,2-dimethylcyclohexane contains axial C−H bonds on the two tertiary carbons in its most stable chair conformation. This hinders the approach of external molecules and consequently leads to more oxidation on the secondary carbon atoms relative to the *cis* isomer.

The previously reported catalyst $[Fe(bpmen)(OTf)_2]$ was also investigated on the basis of its similarly strong preference for hydroxylation.[29,46,47,49−52] The bpmen compound promotes the oxidation of C−H bonds on tertiary carbons over those on secondary carbons when the substrate is *cis*-1,2-dimethylcyclohexane (Table 4). This result is anticipated from consideration of the bond dissociation energies (BDEs). The C−H bonds on tertiary carbons should have BDEs approximately 3 kcal mol^{-1} lower than those on secondary carbons;[53] the bonds on the tertiary carbons should and often do react more quickly as a consequence.[44,47,54−56] Upon reaction with the *trans* isomer, activation of the C−H bonds on secondary carbons is favored, albeit slightly. Similar results are observed for $[Fe(bpmcn)(MeCN)_2]^{2+}$, which has methyl groups in place of the bbpc ligand's benzyl groups. The bpmcn catalyst is less active under these conditions but exhibits a noticeably higher preference for the C−H bonds on secondary carbons. When the ligand is switched to pdp, the preference for oxidizing the bonds on secondary carbons is likewise stronger than that of the bpmen system (Table 4).[13] The bbpc complex with Fe(II) favors the oxidation of secondary carbons over tertiary carbons to a greater extent than the other three Fe(II) compounds with both the *cis* and *trans*-1,2-dimethylcyclohexane substrates. With both alkanes, the reactivity of $[Fe(bbpc)(MeCN)_2]^{2+}$ is lower than that of the pdp complex, which is the most active of the four. The reactivity at the tertiary carbons is, however, curtailed to a much larger extent.

The same trend is observed for adamantane (Scheme 3 and Table S2, Supporting Information). Although the observed 5:1 ratio of tertiary/secondary oxidation is unimpressive relative to those found for the 1,2-dimethylcyclohexane reactions, such ratios are commonly much higher for reactions catalyzed by mononuclear nonheme iron complexes.[47] 1,1-Dimethylcyclohexane and *tert*-butylcyclohexane were also investigated using

dx.doi.org/10.1021/ic201695a | Inorg. Chem. 2011, 50, 12651−12660

Table 4. Catalytic Oxidation of *cis*- and *trans*-1,2-Dimethylcyclohexane[a]

substrate	catalyst	overall yield, individual product yields
cis-	$[Fe(bpmen)(OTf)_2]$	45%, *trans*-1,2-dimethylcyclohexanol 31.9% *cis*-1,2-dimethylcyclohexanol 1.1% *cis*-2,3-dimethylcyclohexanone 5% *cis*-3,4-dimethylcyclohexanone 7% **[tertiary/secondary] = 2.8: 1**
trans-	$[Fe(bpmen)(OTf)_2]$	30%, *cis*-1,2-dimethylcyclohexanol 11.3% *trans*-1,2-dimethylcyclohexanol 0.7% *trans*-2,3-dimethylcyclohexanone 11% *trans*-3,4-dimethylcyclohexanone 7% **[tertiary/secondary] = 1: 1.5**
cis-	$[Fe(bpmcn)(MeCN)_2](SbF_6)_2$	37%, *trans*-1,2-dimethylcyclohexanol 24% *cis*-2,3-dimethylcyclohexanone 5% *cis*-3,4-dimethylcyclohexanone 8% **[tertiary/secondary] = 1.8: 1**
trans-	$[Fe(bpmcn)(MeCN)_2](SbF_6)_2$	20%, *cis*-1,2-dimethylcyclohexanol 7% *trans*-2,3-dimethylcyclohexanone 6% *trans*-3,4-dimethylcyclohexanone 7% **[tertiary/secondary] = 1: 1.9**
cis-	$[Fe(pdp)(MeCN)_2](SbF_6)_2$	70%, *trans*-1,2-dimethylcyclohexanol 55% *cis*-2,3-dimethylcyclohexanone 9% *cis*-3,4-dimethylcyclohexanone 6% **[tertiary/secondary] = 4: 1**
trans-	$[Fe(pdp)(MeCN)_2](SbF_6)_2$	79%, *cis*-1,2-dimethylcyclohexanol 29% *trans*-2,3-dimethylcyclohexanone 22% *trans*-3,4-dimethylcyclohexanone 28% **[tertiary/secondary] = 1: 1.7**
cis-	$[Fe(bbpc)(MeCN)_2](SbF_6)_2$	32%, *trans*-1,2-dimethylcyclohexanol 16.1% *cis*-1,2-dimethylcyclohexanol 0.9% *cis*-2,3-dimethylcyclohexanone 7% *cis*-3,4-dimethylcyclohexanone 5% **[tertiary/secondary] = 1.4: 1**
trans-	$[Fe(bbpc)(MeCN)_2](SbF_6)_2$	29%, *cis*-1,2-dimethylcyclohexanol 4.4% *trans*-1,2-dimethylcyclohexanol 0.6% *trans*-2,3-dimethylcyclohexanone 11% *trans*-3,4-dimethylcyclohexanone 13% **[tertiary/secondary] = 1: 4.8**

[a]Standard reaction conditions: the general procedure was adapted from ref 13 in order to facilitate direct comparison of the data. The substrate (0.056 g, 0.50 mmol, 1 equiv) was dissolved in 1.0 mL of MeCN. The iron catalyst and the terminal oxidant, H_2O_2, were added to this solution in three portions. For each addition, the H_2O_2 was added dropwise over the course of 90 s. After the first additions, the concentrations were as follows: [Fe] = 4.26 μM, [substrate] = 85.2 μM, [H_2O_2] = 0.102 mM. Ten minutes after the first portion of H_2O_2 was added, further equivalents of catalyst and oxidant were added, yielding the following concentrations: [Fe] = 4.65 μM, [substrate] = 46.5 μM, [H_2O_2] = 0.112 mM. Twenty minutes after the first portion of H_2O_2 was added, the third portions of catalyst and oxidant were added, yielding the following concentrations: [Fe] = 4.80 μM, [substrate] = 32.0 μM, [H_2O_2] = 0.115 mM. At 30 min, the reaction solution was filtered through a short plug of silica gel to remove the metal complexes. Cyclohexanone was added as an internal standard, and the products were analyzed using GC. The products were identified through a comparison of the GC retention times and mass spectra (GC/MS) to those of commercially available or previously prepared standards.[13,44,47] All data are the averages of three independent runs.

Chen and White's protocol (Scheme 3 and Table S2, Supporting Information). With *tert*-butylcyclohexane, oxidation is observed at neither the tertiary carbon nor the secondary carbons α to the tertiary carbon. With 1,1-dimethylcyclohexane, the plurality of the oxidation occurs at the γ carbon, as opposed to the β carbon for the pdp oxidant.[13] A preference for activating the C−H bonds on primary over secondary carbons is not observed. Oxidation of the methyl groups of the dimethylcyclohexane substrates is not seen. Additionally, when *n*-hexane is used as a substrate, oxygenation occurs exclusively on the secondary carbon atoms in the chain (Table S2, Supporting Information).

Characterization of a Reactive Intermediate. When 4 equiv of H_2O_2 are allowed to react with $[Fe(bbpc)(MeCN)_2]^{2+}$ in MeCN in the absence of a hydrocarbon substrate, the solution turns green with an optical feature at 690 nm (Figure 4). At room temperature, the solution quickly turns blue, concomitant with the appearance of a new absorbance band at 640 nm. The compound associated with the 640 nm species has not yet been fully characterized. The addition of 20 equiv of $HClO_4$ to the solution prolongs the lifetime of the green species, whereas the addition of Et_3N immediately leads to the loss of the 690 nm band. EPR analysis of a sample quenched during the decay process shows two signals (Figure 5). One has a *g* value equal to 4.3, which is indicative of a high-spin Fe(III) species. The other

Scheme 3

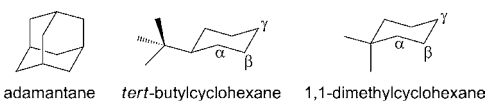

adamantane *tert*-butylcyclohexane 1,1-dimethylcyclohexane

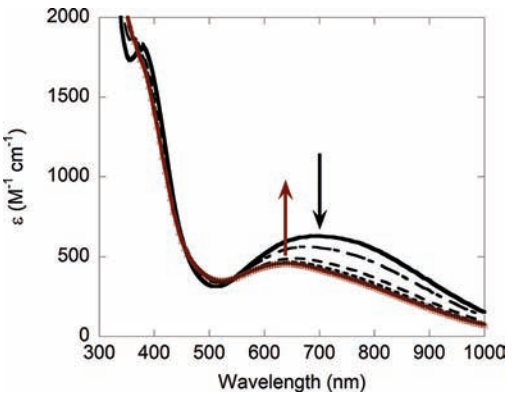

Figure 4. Decay of the green intermediate, tentatively assigned as $[Fe(bbpc)(OOH)]^{2+}$, over time in MeCN at 294 K. The intermediate was generated from the reaction of 1.0 mM $[Fe(bbpc)(MeCN)_2](SbF_6)_2$ with 4.0 equiv of H_2O_2. The lower limit for the ε of the 690 nm feature is 650 M^{-1} cm^{-1}; when 20 equiv of $HClO_4$ are added, the ε increases to 740 M^{-1} cm^{-1} (not shown). Six spectra are displayed; from top to bottom, these were acquired at t = 24 s (dark black), 60 s, 120 s, 180 s, 240 s, and 300 s (dark red), with t = 0 s corresponding to the initial reaction between H_2O_2 and Fe(II).

dx.doi.org/10.1021/ic201695a | *Inorg. Chem.* 2011, 50, 12651–12660

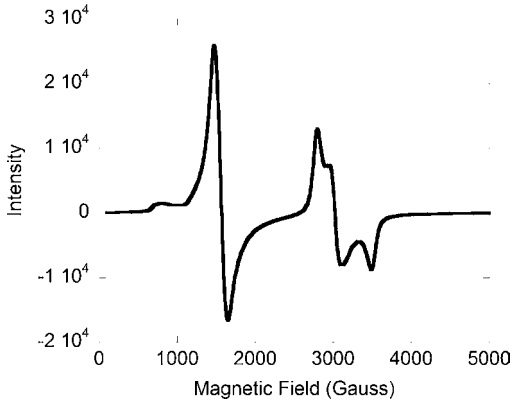

Figure 5. X-band EPR spectrum of the green intermediate, tentatively assigned as $[Fe(bbpc)(OOH)]^{2+}$, as a frozen MeCN solution at 77 K. The sample was prepared from the reaction between 1.0 mM

signal is consistent with a low-spin Fe(III) complex, with g values at 2.36, 2.22, and 1.92 (Figure 5). A mass spectrum of the complex has a major m/z peak consistent with $[Fe(bbpc)(O_2)]^+$ (Figures S8 and S9, Supporting Information). On the basis of the reactivity of the 690 nm species with the acid and base and comparison of the spectroscopic features to previously reported species, we tentatively assign the green species associated with the 690 nm band as $[Fe(bbpc)(OOH)]^{2+}$.

DISCUSSION

The ligand *N*,*N*′-di(phenylmethyl)-*N*,*N*′-bis(2-pyridinylmethyl)-1,2-cyclohexanediamine (bbpc) was prepared as a bulkier analog of bpmcn and bpmen (Scheme 1), which were previously reported to support nonheme iron C−H activation chemistry.[29,32,46,49−52,56−58] Large quantities of crystalline bbpc (Figure S1, Supporting Information) can be prepared within a reasonable time frame without the need for chromatography. The ligand chelates metals ions readily, despite the additional steric bulk, and complexes with both Mn(II) and Fe(II) can be obtained in moderate yield (45−65%).

Much like bpmcn, the ligand can chelate transition metal ions in multiple fashions.[32] In two of the Fe(II) structures (Figure 1) and the lone Mn(II) structure (Figure S2, Supporting Information), the *cis*-α conformation is observed. The nearly eclipsed conformation between Fe−Cl(2) and the benzyl group on N(4) is associated with the much longer Fe−Cl(2) and Fe−N(4) bonds within $[Fe(bbpc)Cl_2]$ (Table 2). The *trans* conformer is observed in the disordered structure of $[Fe(bbpc)(OTf)_2]$ (Figure 2). To the best of our knowledge, this is the first instance of this particular conformation in the coordination chemistry of bpmcn or its close derivatives, which were previously found to coordinate metal ions in *cis*-α and *cis*-β conformations.[35,59−64] The novel mode of coordination may be facilitated by the larger substituents on the amines, but the energetic rationale is not obvious from a precursory inspection of the structure. The conformation of the ligand in $[Fe(bbpc)(OTf)_2]$ places the benzyl groups on the same side of the plane defined by the four N-donors. With this configuration, the benzyl groups strongly repel the disordered triflate, as indicated by the longer Fe−O(1) bond. This would be anticipated to destabilize the structure, although this may be counterbalanced by the reduced steric interactions around the second triflate.

The $[Fe(bbpc)(MeCN)_2](SbF_6)_2$ and $[Fe(bbpc)(OTf)_2]$ compounds have different UV/vis spectra in MeCN (Figure S3, Supporting Information), indicating that the same iron complex is not present in solution. That the spectra differ is likely a consequence of the two different ligand conformations, which appear to be static on the NMR time scale. Another contributing factor may be the possibility of the triflate ions' continued coordination to the Fe(II) center in solution. These ions are capable of binding to the Fe(II), as seen in Figure 2 and the crystal structures of other ferrous complexes with neutral polydentate ligands.[46,65]

The three Fe(II) compounds were investigated as catalysts for alkane oxidation, using the oxidation of cyclohexane by H_2O_2 as a standard reaction (Table 3). The $[Mn(bbpc)Cl_2]$ complex was also investigated but was not found to be a competent catalyst for the reaction. The catalytic activities of the iron compounds scale inversely with the binding affinities of the monodentate anions, and the most strongly coordinating anion, Cl^-, leads to the weakest activity. Similar counteranion dependencies have been previously observed in the hydrocarbon oxidation catalyzed by nonheme iron compounds.[66−69] The most straightforward explanation for this behavior is that the counterions are competing with the terminal oxidant for coordination sites on the metal, slowing the metal oxidation step of the relevant catalytic cycle or cycles. The continued presence of an anionic ligand on the iron may also serve to destabilize any higher-valent oxidants which form during the catalysis.[70] As observed by Costas and Que, the ligand conformation can impact the reactivity profile.[32] That the catalytic activity of $[Fe(bbpc)(OTf)_2]$ (*trans*) is intermediate between those of $[Fe(bbpc)Cl_2]$ and $[Fe(bbpc)(MeCN)_2]^{2+}$ (*cis*-α) may therefore be coincidental.

With cyclohexane as a substrate, the ratio of alcohol (A) to ketone (K) products is relatively high for $[Fe(bbpc)(MeCN)_2]^{2+}$, particularly at lower loadings of the terminal oxidant, H_2O_2.[43,44] Although the preference for hydroxylation is strong relative to most nonheme iron catalysts, higher A/K ratios are found for $[Fe(bpmen)(OTf)_2]$, $[Fe(^{Me2}PyTACN)(OTf)_2]$, and two iron complexes with electronically and sterically modified bpmen ligands.[32,33,45,55,71,72] When acetic acid (AcOH) is added as a stoichiometric additive, the A/K ratio increases from 7.3 to 12.1 with 10 equiv of H_2O_2 (Table 3). Under these conditions, $[Fe(bbpc)(MeCN)_2]^{2+}$ essentially matches $[Fe(^{Me2}PyTACN)(OTf)_2]$ with respect to the selectivity for hydroxylation, although the latter system is about twice as active, with a 65% oxidative efficiency relative to the 28% for the bbpc system. Although AcOH has been previously found to improve both the selectivity of iron-mediated epoxidation reactions[49] and the regioselectivity of iron-mediated hydrocarbon oxidation reactions,[13,44] the ability to hinder the formation of ketones in alkane oxygenation reactions had not been noted. The loss of overall activity upon the addition of AcOH contrasts with a previously reported titanium catalyst, which was found to catalyze the oxidation of cyclohexane by hydrogen peroxide to a much higher degree when the reaction was run in AcOH,[73] as well as a nonheme iron system reported by Chen and White.[17]

The addition of AcOH slows the oxidation of cyclohexanol to cyclohexanone as shown in Figure 3, accounting for the higher A/K ratio. Analysis of the curve yields a surprising result in that AcOH has little impact on the lifetime of the catalytic activity (Figure S7, Supporting Information), with the estimated half-life increasing by approximately 1 min. We therefore hypothesize that the AcOH is either decreasing the intrinsic reactivity of the generated oxidant(s) or reversibly deactivating it, as opposed to

dx.doi.org/10.1021/ic201695a | *Inorg. Chem.* 2011, 50, 12651−12660

hastening the irreversible degradation of one or more species in the catalytic cycle. Whether the loss of activity is a consequence of the acidity or the metal-binding properties of AcOH remains unresolved. The protonation of M(IV) oxo species has recently been found to slow their C−H activation chemistry.[58,74]

The increased steric bulk was designed to direct oxidation toward the less sterically congested portions of hydrocarbon substrates. In order to test this, we adopted a protocol developed by Chen and White to test the regioselectivity of the alkane oxidation catalyzed by $[Fe(pdp)(MeCN)_2]^{2+}$.[13] Under these conditions, which use a lower loading of substrate, the C−H bonds on secondary carbons are oxidized predominantly to the ketone instead of the alcohol; when cyclohexane is used as a substrate, 22% of the substrate is converted to a 1:9 mixture of cyclohexanol and cyclohexanone. We analyzed both $[Fe(bbpc)(MeCN)_2]^{2+}$ and $[Fe(bpmen)(OTf)_2]$, with the intention of determining whether there was a correlation between the A/K ratio in the previously described cyclohexane reactivity (Table 3) and the regioselectivity observed with the 1,2-dimethylcyclohexanes (Table 4). We also analyzed $[Fe(bpmcn)(MeCN)_2]^{2+}$ in order to assess how much of the tuned regioselectivity was a consequence of the benzyl-for-methyl substitution.

The Fe(II) complex with bbpc has the strongest preference of the four catalysts for activating C−H bonds on secondary carbons over the thermodynamically weaker ones on tertiary carbons (Table 4). As anticipated, this preference is most pronounced with *tert*-butylcyclohexane and *trans*-1,2-dimethylcyclohexane.[48] With both 1,2-dimethylcyclohexane substrates, the overall reactivity decreases upon switching from the pdp ligand to the bbpc. The oxidation at the tertiary carbons, however, decreases to a much higher degree, going from 55% to 17% conversion for the *cis* isomer and from 29% to 5% for the *trans*. The results are consistent with steric repulsions between the substrate and catalyst regulating and restricting substrate access to the reactive portions of the active oxidant, which may be a higher-valent iron species, such as a ferryl oxo species.[57,75−79] When adamantane is used as a substrate, the ratio of tertiary to secondary oxidation is 5:1, likely due to the greater accessibility of the tertiary C−H bonds relative to those in the cyclohexane derivatives. This ratio is lower than those observed for other mononuclear nonheme iron catalysts, with the exception of $[Fe(N4Py)(MeCN)]^{2+}$, which has a 3.3:1 ratio.[47,80] A similar decrease in the ability to activate tertiary C−H bonds was observed in the oxidation chemistry of iron complexes with methylated derivatives of tris(pyridyl)amine (tpa).[47]

The bpmcn system has a stronger preference for secondary carbon oxidation than $[Fe(bpmen)(OTf)_2]$, suggesting that the substitution of a cyclohexane ring for the ethylene linkage does impact the regioselectivity of the oxidation. However, the benzyl-for-methyl substitution also has a significant impact as assessed by the lower ratios of tertiary to secondary carbon oxidation for the bbpc system relative to $[Fe(bpmcn)(MeCN)_2]^{2+}$. The relative importance of these two perturbations appears to be substrate-dependent. With *cis*-1,2-dimethylcyclohexane, the cyclohexane ring in the bbpc appears to account for the bulk of the altered regioselectivity; for secondary carbon, oxidation accounts for 35% of the oxidized products for $[Fe(bpmcn)(MeCN)_2]^{2+}$ versus 38% for $[Fe(bbpc)(MeCN)_2]^{2+}$. With the *trans* substrate, the benzyl substituents appear to have the stronger influence, with secondary carbon oxidation accounting for 60%, 65%, and 83% of the organic products in the systems using bpmen, bpmcn, and bbpc ligands, respectively.

The ability of steric repulsions to block oxidation at positions α and β to the installed group is more limited (Scheme 3 and Table S2, Supporting Information). The oxidation catalyzed by $[Fe(bbpc)(MeCN)_2]^{2+}$ tends to occur at sites farther from the bulkier portions of the substrates than that catalyzed by $[Fe(pdp)(MeCN)_2]^{2+}$. With *tert*-butylcyclohexane, no oxidation is seen on the secondary carbons α to the *tert*-butyl group. Oxidation on the β carbons is preferred, with a 3.7:1 ratio of β to γ oxidation, but not to the same extent as in Chen and White's pdp system (4.9:1).[13] With 1,1-dimethylcyclohexane, oxidation is observed at the carbons α, β, and γ to the quaternary carbon. With the bbpc ligand, oxidation is favored on the γ, with an $\alpha/\beta/\gamma$ ratio of 1:1.3:2.3. This contrasts with the pdp system, which oxidizes the β position of 1,1-dimethylcyclohexane preferentially, with a $\alpha/\beta/\gamma$ ratio of 1:1.5:0.8.[13]

The steric repulsions do not appear to be sufficient to similarly favor the oxidation of C−H bonds on primary carbons over those on secondary carbons, as illustrated by a lack of primary alcohol and aldehyde products in the oxidations of 1,2-dimethylcyclohexanes and *n*-hexane. The results bolster the previously presented concept that judicious ligand modification can direct the oxidation catalyzed by nonheme iron catalysts toward specific regions of structurally complicated substrates.[13]

There does not appear to be a straightforward correlation between the A/K ratio for cyclohexane oxygenation and the regioselectivity of the 1,2-dimethylcyclohexane oxidation. The $[Fe(bpmen)(OTf)_2]$ complex is slightly more selective for hydroxylation (A/K = 8) than $[Fe(bbpc)(MeCN)_2]^{2+}$, yet it activates the C−H bonds on tertiary carbons much more readily (Table 4). Additionally, $[Fe(^{Me2}PyTACN)(OTf)_2]$ has an even stronger tendency to hydroxylate alkanes (A/K = 12), but only tertiary alcohol products are reported for its oxidation of *cis*-1,2-dimethylcyclohexane.[55] The results suggest that the geometric structure of the catalyst is not solely responsible for the observed preference for hydroxylation.

The tertiary alcohol products display 88−95% stereochemical retention (Table 4). These are comparable to numbers reported for other recently studied nonheme iron systems[44,47] and are inconsistent with a Fenton-style manner of oxidation.[81] In a 2001 paper from Chen and Que, the retention of configuration was found to decrease as the catalyst's ligand was methylated.[47] That the bulkier bbpc ligand leads to less stereochemical retention than bpmen or less sterically hindered derivatives of tpa[47] may suggest that the additional bulk on the ligand may slow oxygen atom rebound steps in the catalytic cycle(s), which would allow intermediate organic radicals more time to rearrange.[57]

Although electronic effects have been found to influence the hydrocarbon oxidation chemistry catalyzed by nonheme iron complexes,[72] we find it more likely that steric effects account for the differences between the bpmcn and bbpc systems. In previous small molecule chemistry, the substitution of a benzyl group for a methyl group was found to have a near negligible impact on the basicity of tertiary amines.[82] Furthermore, the Hammett constants for these two substituents are similar.[83] Recent work by Costas et al. found evidence for a pre-rate-determining step adduct between a high-valent Mn(IV) oxo species and benzylic substrates.[84] They attributed the formation of such adducts to weak hydrogen bonds between the oxo functional group and C−H bonds on the substrates.[84] The influence of the additional steric bulk in the bbpc system may be manifesting itself by limiting the ways in which the substrate can interact with the oxidant, but we are hesitant to

speculate further given that (1) we have not observed an analogous pre-rate-determining step equilibrium and (2) the nature of the relevant oxidant in the catalysis is not yet fully established.

The reactivity appears to proceed through a Fe(III)−OOH species that has an absorption band at 690 nm (Figure 4) and both high-spin and low-spin Fe(III) EPR signals at 77 K (Figure 5). These are similar to spectroscopic features reported for other ferric hydroperoxide species.[79,80,85−87] Although the mass spectrum has a major m/z peak consistent with $[Fe(bbpc)(O_2)]^+$, we find this assignment to be implausible on the basis of the reactivity of the intermediate with $HClO_4$ and Et_3N. On the basis of prior reports involving ferric peroxo species, the addition of $HClO_4$ would convert $[Fe(bbpc)(O_2)]^+$ to $[Fe(bbpc)(OOH)]^{2+}$.[77,79,87] Closely related ferric peroxo and hydroperoxo species have been found to give rise to markedly different optical spectra.[77,87] We see little change in the optical spectrum of the 690 nm intermediate upon the addition of $HClO_4$; further to the contrary, the species appears to be more stable under such conditions. The addition of Et_3N, conversely, would be anticipated to stabilize $[Fe(bbpc)(O_2)]^+$,[76,77,87] which contrasts sharply with the loss of the 690 nm feature that we observe upon adding base. We hypothesize that the m/z feature results from the deprotonation of $[Fe(bbpc)(OOH)]^{2+}$ to a less positively charged species. Ferric hydroperoxide species have previously displayed similar instability under ESI conditions,[29] and the lack of an m/z feature corresponding to $[Fe(bbpc)(OOH)]^{2+}$ should not be considered infallible proof of its absence. The mixture of high-spin and low-spin signals may be indicative of a spin-crossover. Neutral N-donor ligands have supported both high-spin and low-spin Fe(III)−OOH species,[79,85−87] and a recent study with ferric alkylperoxo complexes found that a relatively minor ligand modification could convert a low-spin Fe(III)−OOR species to a high-spin one.[88] Ferric hydroperoxide species have been previously hypothesized and reported to spontaneously convert to higher-valent iron species, such as ferryl oxo complexes.[47,51,55,76,77,89] These more highly oxidized iron species may be the actual oxidants in the alkane oxygenation reactions.[90]

CONCLUSIONS

The bbpc ligand is presented as a more sterically encumbered analog of previously reported tetradentate N-donor ligands that supported nonheme iron oxidative catalysis. The catalytic capabilities of Fe(II) compounds with bbpc are strongly dependent on the counterions employed, with the most active alkane oxidation associated with the most weakly binding counteranion, SbF_6^-. The $[Fe(bbpc)(MeCN)_2]^{2+}$ complex also displays the strongest preference for alkane hydroxylation of the three bbpc complexes, and its selectivity for hydroxylation is on par with that of $[Fe(bpmen)(OTf)_2]$, which has been described as "the prototypical example of an efficient stereospecific alkane hydroxylation catalyst."[55] The preference for hydroxylation is amplified in the presence of stoichiometric acetic acid, albeit with a loss of activity. Last, the benzyl groups and the cyclohexane ring on the catalyst both appear to impede the oxidation of sterically congested C−H bonds. Although the C−H bonds on secondary carbons are still activated readily, those on tertiary carbons are oxidized less avidly than in other reported nonheme iron systems. Further modifications could potentially preclude oxidation at tertiary carbons or even direct oxidation toward primary carbons.

ASSOCIATED CONTENT

Supporting Information

Crystallographic data, ORTEP representations, comparative optical spectroscopy, ^1H NMR spectra, oxidation data, mass spectra, and a comparison of predicted m/z features. This material is available free of charge via the Internet at http://pubs.acs.org.

AUTHOR INFORMATION

Corresponding Author

*E-mail: crgoldsmith@auburn.edu.

ACKNOWLEDGMENTS

This work was funded by Auburn University and a Doctoral New Investigator grant from the American Chemical Society—Petroleum Research Fund. The authors are also grateful to Prof. Evert Duin for his assistance with the acquisition and interpretation of EPR data. This article is dedicated in memoriam to Prof. Cristina M. Coates.

REFERENCES

(1) Shilov, A. E.; Shul'pin, G. B. *Chem. Rev.* **1997**, *97*, 2879−2932.
(2) Lersch, M.; Tilset, M. *Chem. Rev.* **2005**, *105*, 2471−2526.
(3) Davies, H. M. L.; Beckwith, R. E. J. *Chem. Rev.* **2003**, *103*, 2861−2904.
(4) Jia, C.; Kitamura, T.; Fujiwara, Y. *Acc. Chem. Res.* **2001**, *34*, 633−639.
(5) Crabtree, R. H. *Chem. Rev.* **2010**, *110*, 575.
(6) Bhan, A.; Iglesia, E. *Acc. Chem. Res.* **2008**, *41*, 559−567.
(7) De Vos, D. E.; Dams, M.; Sels, B. F.; Jacobs, P. A. *Chem. Rev.* **2002**, *102*, 3615−3640.
(8) Ernst, S.; Disteldorf, H.; Yang, X. *Microporous Mesoporous Mater.* **1998**, *22*, 457−464.
(9) Lee, S. J.; Lin, W. *Acc. Chem. Res.* **2008**, *41*, 521−537.
(10) Fiedler, D.; Leung, D. H.; Bergman, R. G.; Raymond, K. N. *Acc. Chem. Res.* **2004**, *38*, 349−358.
(11) Fackler, P.; Berthold, C.; Voss, F.; Bach, T. *J. Am. Chem. Soc.* **2010**, *132*, 15911−15913.
(12) Das, S.; Incarvito, C. D.; Crabtree, R. H.; Brudvig, G. W. *Science* **2006**, *312*, 1941−1943.
(13) Chen, M. S.; White, M. C. *Science* **2010**, *327*, 566−571.
(14) Goldsmith, C. R.; Coates, C. M.; Hagan, K.; Mitchell, C. A. *J. Mol. Catal. A* **2011**, *335*, 24−30.
(15) Chen, J.; Che, C.-M. *Angew. Chem., Int. Ed.* **2004**, *43*, 4950−4954.
(16) Zhang, J.-L.; Che, C.-M. *Chem.—Eur. J.* **2005**, *11*, 3899−3914.
(17) Chen, M. S.; White, M. C. *Science* **2007**, *318*, 783−787.
(18) Holm, R. H.; Kennepohl, P.; Solomon, E. I. *Chem. Rev.* **1996**, *96*, 2239−2314.
(19) Mirica, L. M.; Ottenwaelder, X.; Stack, T. D. P. *Chem. Rev.* **2004**, *104*, 1013−1046.
(20) Gupta, R.; Borovik, A. S. *J. Am. Chem. Soc.* **2003**, *125*, 13234−13242.
(21) Borovik, A. S. *Acc. Chem. Res.* **2005**, *38*, 54−61.
(22) Gupta, R.; MacBeth, C. E.; Young, V. G. Jr.; Borovik, A. S. *J. Am. Chem. Soc.* **2002**, *124*, 1136−1137.
(23) Parsell, T. H.; Behan, R. K.; Green, M. T.; Hendrich, M. P.; Borovik, A. S. *J. Am. Chem. Soc.* **2006**, *128*, 8728−8729.
(24) MacBeth, C. E.; Golombek, A. P.; Young, V. G. Jr.; Yang, C.; Kuczera, K.; Hendrich, M. P.; Borovik, A. S. *Science* **2000**, *289*, 938−941.
(25) Lacy, D. C.; Gupta, R.; Stone, K. L.; Greaves, J.; Ziller, J. W.; Hendrich, M. P.; Borovik, A. S. *J. Am. Chem. Soc.* **2010**, *132*, 12188−12190.
(26) Klinker, E. J.; Kaizer, J.; Brennessel, W. W.; Woodrum, N. L.; Cramer, C. J.; Que, L. Jr. *Angew. Chem., Int. Ed.* **2005**, *44*, 3690−3694.
(27) England, J.; Guo, Y.; Farquhar, E. R.; Young, V. G. Jr.; Münck, E.; Que, L. Jr. *J. Am. Chem. Soc.* **2010**, *132*, 8635−8644.

(28) Rohde, J.-U.; In, J.-H.; Lim, M. H.; Brennessel, W. W.; Bukowski, M. R.; Stubna, A.; Münck, E.; Nam, W.; Que, L. Jr. *Science* **2003**, *299*, 1037−1039.
(29) Chen, K.; Costas, M.; Kim, J.; Tipton, A. K.; Que, L. Jr. *J. Am. Chem. Soc.* **2002**, *124*, 3026−3035.
(30) Cook, B. R.; Reinert, T. J.; Suslick, K. S. *J. Am. Chem. Soc.* **1986**, *108*, 7281−7286.
(31) Groves, J. T.; Viski, P. *J. Am. Chem. Soc.* **1989**, *111*, 8537−8538.
(32) Costas, M.; Que, L. Jr. *Angew. Chem., Int. Ed.* **2002**, *41*, 2179−2181.
(33) Mekmouche, Y.; Ménage, S.; Pécaut, J.; Lebrun, C.; Reilly, L.; Schuenemann, V.; Trautwein, A.; Fontecave, M. *Eur. J. Inorg. Chem.* **2004**, *2004*, 3163−3171.
(34) Haynes, J. S.; Sams, J. R.; Thompson, R. C. *Can. J. Chem.* **1981**, *59*, 669−678.
(35) Glerup, J.; Goodson, P. A.; Hazell, A.; Hazell, R.; Hodgson, D. J.; McKenzie, C. J.; Michelsen, K.; Rychlewska, U.; Toftlund, H. *Inorg. Chem.* **1994**, *33*, 4105−4111.
(36) Stoll, S.; Schweiger, A. *J. Magn. Reson.* **2006**, *178*, 42−55.
(37) Sheldrick, G. M. *SHELXTL*, 6.12 ed.; Siemens Analytical X-ray Instruments, Inc.: Madison, WI, 2001.
(38) Sheldrick, G. M. *SADABS*; Bruker Analytical X-ray Systems: Madison, WI, 1996.
(39) Fenton, R. R.; Vagg, R. S.; Jones, P.; Williams, P. A. *Inorg. Chim. Acta* **1987**, *128*, 219−229.
(40) Coates, C. M.; Hagan, K.; Mitchell, C. A.; Gorden, J. D.; Goldsmith, C. R. *Dalton Trans.* **2011**, *40*, 4048−4058.
(41) Shannon, R. D. *Acta Crystallogr.* **1976**, *A32*, 751−767.
(42) Goldsmith, C. R.; Jonas, R. T.; Cole, A. P.; Stack, T. D. P. *Inorg. Chem.* **2002**, *41*, 4642−4652.
(43) Tanase, S.; Marques-Gallego, P.; Browne, W. R.; Hage, R.; Bouwman, E.; Feringa, B. L.; Reedijk, J. *Dalton Trans.* **2008**, 2026−2033.
(44) Gómez, L.; Garcia-Bosch, I.; Company, A.; Benet-Buchholz, J.; Polo, A.; Sala, X.; Ribas, X.; Costas, M. *Angew. Chem., Int. Ed.* **2009**, *48*, 5720−5723.
(45) England, J.; Britovsek, G. J. P.; Rabadia, N.; White, A. J. P. *Inorg. Chem.* **2007**, *46*, 3752−3767.
(46) Britovsek, G. J. P.; England, J.; White, A. J. P. *Inorg. Chem.* **2005**, *44*, 8125−8134.
(47) Chen, K.; Que, L. Jr. *J. Am. Chem. Soc.* **2001**, *123*, 6327−6337.
(48) Newhouse, T.; Baran, P. S. *Angew. Chem., Int. Ed.* **2011**, *50*, 3362−3374.
(49) Mas-Ballesté, R.; Que, L. Jr. *J. Am. Chem. Soc.* **2007**, *129*, 15964−15972.
(50) Quiñonero, D.; Musaev, D. G.; Morokuma, K. *Inorg. Chem.* **2003**, *42*, 8449−8455.
(51) Quiñonero, D.; Morokuma, K.; Musaev, D. G.; Mas-Ballesté, R.; Que, L. Jr. *J. Am. Chem. Soc.* **2005**, *127*, 6548−6549.
(52) Kim, S. O.; Sastri, C. V.; Seo, M. S.; Kim, J.; Nam, W. *J. Am. Chem. Soc.* **2005**, *127*, 4178−4179.
(53) McMillen, D. F.; Golden, D. M. *Annu. Rev. Phys. Chem.* **1982**, *33*, 493−532.
(54) Goldsmith, C. R.; Jonas, R. T.; Stack, T. D. P. *J. Am. Chem. Soc.* **2002**, *124*, 83−96.
(55) Company, A.; Gómez, L.; Güell, M.; Ribas, X.; Luis, J. M.; Que, L. Jr.; Costas, M. *J. Am. Chem. Soc.* **2007**, *129*, 15766−15767.
(56) Kaizer, J.; Klinker, E. J.; Oh, N. Y.; Rohde, J.-U.; Song, W. J.; Stubna, A.; Kim, J.; Münck, E.; Nam, W.; Que, L. Jr. *J. Am. Chem. Soc.* **2004**, *126*, 472−473.
(57) Nam, W. *Acc. Chem. Res.* **2007**, *40*, 522−531.
(58) Fiedler, A. T.; Que, L. Jr. *Inorg. Chem.* **2009**, *48*, 11038−11047.
(59) Murphy, A.; Dubois, G.; Stack, T. D. P. *J. Am. Chem. Soc.* **2003**, *125*, 5250−5251.
(60) Costas, M.; Tipton, A. K.; Chen, K.; Jo, D.-H.; Que, L. Jr. *J. Am. Chem. Soc.* **2001**, *123*, 6722−6723.
(61) Costas, M.; Rohde, J.-U.; Stubna, A.; Ho, R. Y. N.; Quaroni, L.; Münck, E.; Que, L. Jr. *J. Am. Chem. Soc.* **2001**, *123*, 12931−12932.
(62) Wu, M.; Wang, B.; Wang, S.; Xia, C.; Sun, W. *Org. Lett.* **2009**, *11*, 3622−3625.
(63) Birse, E. F.; Cox, M. A.; Williams, P. A.; Stephens, F. S.; Vagg, R. S. *Inorg. Chim. Acta* **1988**, *148*, 45−56.
(64) Reynolds, M. F.; Costas, M.; Ito, M.; Jo, D.-H.; Tipton, A. A.; Whiting, A. K.; Que, L. Jr. *J. Biol. Inorg. Chem.* **2003**, *8*, 263−272.
(65) Mas-Ballesté, R.; Costas, M.; van den Berg, T.; Que, L. Jr. *Chem.—Eur. J.* **2006**, *12*, 7489−7500.
(66) White, M. C.; Doyle, A. G.; Jacobsen, E. N. *J. Am. Chem. Soc.* **2001**, *123*, 7194−7195.
(67) Sastri, C. V.; Lee, J.; Oh, K.; Lee, Y. J.; Lee, J.; Jackson, T. A.; Ray, K.; Hirao, H.; Shin, W.; Halfen, J. A.; Kim, J.; Que, L. Jr.; Shaik, S.; Nam, W. *Proc. Natl. Acad. Sci., U. S. A.* **2007**, *104*, 19181−19186.
(68) Leising, R. A.; Norman, R. E.; Que, L. Jr. *Inorg. Chem.* **1990**, *29*, 2553−2555.
(69) Kim, C.; Chen, K.; Kim, J.; Que, L. Jr. *J. Am. Chem. Soc.* **1997**, *119*, 5964−5965.
(70) Rohde, J.-U.; Stubna, A.; Bominaar, E. L.; Münck, E.; Nam, W.; Que, L. Jr. *Inorg. Chem.* **2006**, *45*, 6435−6445.
(71) Chen, K.; Que, L. Jr. *Chem. Commun.* **1999**, 1375−1376.
(72) England, J.; Gondhia, R.; Bigorra-Lopez, L.; Petersen, A. R.; White, A. J. P.; Britovsek, G. J. P. *Dalton Trans.* **2009**, 5319−5334.
(73) Sooknoi, T.; Limtrakul, J. *Appl. Catal., A* **2002**, *233*, 227−237.
(74) Shi, S.; Wang, Y.; Xu, A.; Wang, H.; Zhu, D.; Roy, S. B.; Jackson, T. A.; Busch, D. H.; Yin, G. *Angew. Chem., Int. Ed.* **2011**, *50*, 7321−7324.
(75) Que, L. Jr. *Acc. Chem. Res.* **2007**, *40*, 493−500.
(76) Lee, Y.-M.; Hong, S.; Morimoto, Y.; Shin, W.; Fukuzumi, S.; Nam, W. *J. Am. Chem. Soc.* **2010**, *132*, 10668−10670.
(77) Li, F.; Meier, K. K.; Cranswick, M. A.; Chakrabarti, M.; Van Heuvelen, K. M.; Münck, E.; Que, L. Jr. *J. Am. Chem. Soc.* **2011**, *133*, 7256−7259.
(78) Mukherjee, A.; Cranswick, M. A.; Chakrabarti, M.; Paine, T. K.; Fujisawa, K.; Münck, E.; Que, L. Jr. *Inorg. Chem.* **2010**, *49*, 3618−3628.
(79) Martinho, M.; Blain, G.; Banse, F. *Dalton Trans.* **2010**, *39*, 1630−1634.
(80) Roelfes, G.; Lubben, M.; Hage, R.; Que, L. Jr.; Feringa, B. L. *Chem.—Eur. J.* **2000**, *6*, 2152−2159.
(81) Russell, G. A. *J. Am. Chem. Soc.* **1957**, *79*, 3871−3877.
(82) Goldsmith, C. R.; Lippard, S. J. *Inorg. Chem.* **2006**, *45*, 6474−6478.
(83) Isaacs, N. S. *Physical Organic Chemistry*, 2nd ed.; John Wiley & Sons Inc.: New York, 1995.
(84) Garcia-Bosch, I.; Company, A.; Cady, C. W.; Styring, S.; Browne, W. R.; Ribas, X.; Costas, M. *Angew. Chem., Int. Ed.* **2011**, *50*, 5648−5653.
(85) Roelfes, G.; Lubben, M.; Chen, K.; Ho, R. Y. N.; Meetsma, A.; Genseberger, S.; Hermant, R. M.; Hage, R.; Mandal, S. K.; Young, V. G. Jr.; Zang, Y.; Kooijman, H.; Spek, A. L.; Que, L. Jr.; Feringa, B. L. *Inorg. Chem.* **1999**, *38*, 1929−1936.
(86) Shearer, J.; Scarrow, R. C.; Kovacs, J. A. *J. Am. Chem. Soc.* **2002**, *124*, 11709−11717.
(87) Ho, R. Y. N.; Roelfes, G.; Hermant, R.; Hage, R.; Feringa, B. L.; Que, L. Jr. *Chem. Commun.* **1999**, 2161−2162.
(88) Namuswe, F.; Hayashi, T.; Jiang, Y.; Kasper, G. D.; Narducci Sarjeant, A. A.; Moënne-Loccoz, P.; Goldberg, D. P. *J. Am. Chem. Soc.* **2009**, *132*, 157−167.
(89) Bassan, A.; Blomberg, M. R. A.; Siegbahn, P. E. M.; Que, L. Jr. *J. Am. Chem. Soc.* **2002**, *124*, 11056−11063.
(90) Park, M. J.; Lee, J.; Suh, Y.; Kim, J.; Nam, W. *J. Am. Chem. Soc.* **2006**, *128*, 2630−2634.

NOTE ADDED AFTER ASAP PUBLICATION

This paper was published on the Web on November 9, 2011. Additional text corrections were implemented and the corrected version was reposted on November 11, 2011.